Author Manuscript

Author Manuscript

Author Manuscript

Author Manuscript

HHS Public Access

Author manuscript

*Nat Immunol*. Author manuscript; available in PMC 2015 March 01.

Published in final edited form as:

*Nat Immunol*. 2014 September ; 15(9): 833–838. doi:10.1038/ni.2957.

# Activation of a G protein-coupled receptor by its endogenous ligand triggers the *Caenorhabditis elegans* innate immune response

**Olivier Zugasti**[1,2,3], **Neelanjan Bose**[4], **Barbara Squiban**[1,2,3,†], **Jérôme Belougne**[1,2,3], **C. Léopold Kurz**[1,2,3,†], **Frank C. Schroeder**[4], **Nathalie Pujol**[1,2,3], and **Jonathan J. Ewbank**[1,2,3]

[1]Centre d'Immunologie de Marseille-Luminy, UM2 Aix-Marseille Université, Case 906, 13288 Marseille cedex 9, France

[2]INSERM, U1104, 13288 Marseille, France

[3]CNRS, UMR7280, 13288 Marseille, France

[4]Boyce Thompson Institute and Department of Chemistry and Chemical Biology, Cornell University, Ithaca, New York 14853, USA

## Abstract

Immune defenses are triggered by microbe-associated molecular patterns or as a result of damage to host cells. The elicitors of immune responses in the nematode *Caenorhabditis elegans* are unclear. Using a genome-wide RNAi screen, we identify the G-protein coupled receptor (GPCR) DCAR-1 as being required for the response to fungal infection and wounding. DCAR-1 acts in the epidermis to regulate the expression of antimicrobial peptides via a conserved p38 mitogen-activated protein kinase pathway. Through targeted metabolomics analysis we identify the tyrosine-derivative 4-hydroxyphenyllactic acid (HPLA) as an endogenous ligand. These findings reveal DCAR-1 and its cognate ligand HPLA to be important triggers of the epidermal innate immune response in *C. elegans* and highlight the ancient role of GPCRs in host defense.

## INTRODUCTION

The innate defenses of the nematode *C. elegans* have diverged significantly from those of other animals. Perhaps most strikingly, *C. elegans* has lost the transcription factor NF-κB,

Users may view, print, copy, and download text and data-mine the content in such documents, for the purposes of academic research, subject always to the full Conditions of use:http://www.nature.com/authors/editorial_policies/license.html#terms

Correspondence and requests for materials should be addressed to O.Z. or J.J.E. (zugasti@ciml.univ-mrs.fr; ewbank@ciml.univ-mrs.fr).

†Current addresses: Section of Hematology/Oncology, Department of Pediatrics, University of Oklahoma Health Sciences Center (BS); Institut de Biologie du Développement de Marseille-Luminy, CNRS, UMR6216, Case 907, 13009 Marseille, France (CLK).

**Author Contributions** O.Z. designed and performed the RNAi screen and most other experiments, analysed and interpreted the data and helped to write the manuscript. B.S., J.B., and C.L.K. performed the RNAi screen, analysed and interpreted the data and reviewed the manuscript. N.B and F.C.S. designed and performed the mass spectrometric analyses, analysed and interpreted data and helped write the manuscript. N.P. designed experiments, analysed and interpreted data and helped write the manuscript. J.J.E. conceived and supervised the project, designed experiments, analysed and interpreted the data and wrote the manuscript.

**COMPETING FINANCIAL INTERESTS**

The authors declare no competing financial interests.

Author Manuscript Author Manuscript Author Manuscript Author Manuscript

key for defense in most animal species, and lacks functional orthologs of many known innate defenses receptors[1]. On the other hand, core-signaling pathways that play roles in innate immunity across a broad range of animal species are conserved in *C. elegans*[2,3], and studies with this genetically tractable model can give insights into mammalian immunity[4,5]. One emerging aspect of molecular conservation in innate immunity concerns G protein-coupled receptors (GPCR). Specific GPCRs can detect bacterially-derived signals and regulate immunity in flies, mice and humans[6–9]. In *C. elegans*, several GPCR genes, including *npr-1*[10] and *fshr-1*[11] are important for host resistance to infection. *npr-1* modulates resistance indirectly[10], and for *fshr-1* the precise mode of function and endogenous ligand is currently unknown. If the capacity to recognize perturbations of the worm's normal cellular physiology, such as a block in protein translation, has been linked to innate immunity[12–14], a full understanding of how pathogens trigger an immune response in *C. elegans* remains elusive[15,16].

One model of nematode infection involves the endoparasitic fungus *Drechmeria coniospora*[17]. Fungal conidia adhere to the worm's cuticle, germinate, penetrate the cuticle and send hyphae throughout the worm. This provokes a rapid innate immune response, including the up-regulation in the epidermis of antimicrobial peptide (AMP) genes such as *nlp-29*[18], one of a cluster of six infection-inducible *nlp* genes[19]. These genes are also induced by sterile wounding[20]. In both cases, AMP expression is principally controlled by a conserved p38 mitogen-activated protein kinase (MAPK) cassette involving *pmk-1*[19,20], also important for the regulation of intestinal defences[3,16]. For epidermal defenses, we previously demonstrated that this signaling cassette acts upstream of the STAT-like transcription factor STA-2[21] and downstream of the protein kinase C (PKC) TPA-1 and the Gα protein GPA-12[22]. This suggests that epidermal innate immune responses are regulated by a GPCR.

Through a functional genomic screen, we identified a single GPCR, DCAR-1, as being required for the expression of antimicrobial peptides upon fungal infection and wounding. DCAR-1 acts via a conserved p38 MAPK pathway in the epidermis and controls resistance to *D. coniospora* infection. We identify 4-hydroxyphenyllactic acid (HPLA) as an endogenous ligand for DCAR-1. Our study thus constitutes the first identification of a receptor-ligand pair controlling innate immunity *C. elegans*.

## RESULTS

### A GPCR required for antifungal innate immunity

A previous demonstration of the involvement of the Gα protein GPA-12 in the regulation of AMP gene expression[22] implicated a role for a unknown GPCR (Fig. 1a). In order to identify this GPCR, as part of a genome-wide screen (unpublished results), using RNA-mediated interference (RNAi) we knocked down individually 1,150 GPCR genes, corresponding to three-quarters of all GPCR genes in *C. elegans* (Supplementary Table 1). We quantified the effect of each RNAi clone on the expression of an AMP reporter gene, *nlp-29p::gfp*[20], following infection with *D. coniospora*, using a semi-automated screening method[23]. We identified only 3 clones, targeting *dcar-1*, *frpr-11* and *srv-21*, that reproducibly decreased reporter gene expression. Unlike *frpr-11*(*RNAi*) and *srv-21(RNAi)*, *dcar-1(RNAi)* did not affect the strong expression of *nlp-29p::gfp* seen in worms expressing

Author Manuscript Author Manuscript Author Manuscript Author Manuscript

a constitutively active form of the Gα protein GPA-12 (GPA-12*)[22,24], suggesting that *dcar-1* alone acts upstream or in parallel to GPA-12. Further, *dcar-1(RNAi)* did not abrogate the induction of *nlp-29* expression provoked by osmotic-stress, which is mediated by a parallel pathway, which is essentially *pmk-1* independent[19] and independent of *gpa-12*[21,22] (Fig. 1a and 1b). These results were recapitulated in a *dcar-1(tm2484)* null mutant[25] background (Fig. 1c and Supplementary Fig. 1).

When we measured the level of gene expression at the *nlp-29* cluster in *dcar-1(tm2484)* and in a second deletion allele *dcar-1(nj66)*[25], we found that loss of *dcar-1* function had a profound effect on the induction of the 6 *nlp* genes after infection, while not affecting their constitutive expression (Fig. 1d,e). Further, *dcar-1* mutants exhibited a markedly heightened susceptibility to *D. coniospora* infection, while at the same time exhibiting essentially wild-type development and longevity on non-pathogenic *E. coli*, as well as normal resistance to the intestinal bacterial pathogen *Pseudomonas aeruginosa* (Fig. 2 and results not shown). Thus, of the 1,150 GPCR genes assayed, *dcar-1* emerged alone as an innate immune receptor gene acting upstream of (or in parallel to) *gpa-12* to regulate of a cluster of epidermal innate immune effector genes and resistance to fungal infection.

## DCAR-1 can be activated by an endogenous ligand

*dcar-1* mutant worms also exhibited an almost complete block of *nlp-29p::gfp* induction following physical injury (Fig. 1c and Supplementary Fig. 1), demonstrating that *dcar-1* can be activated in the absence of a pathogen, and suggesting that its ligand is endogenous. To explore this possibility further, we made use of 2 Dumpy (Dpy) mutants with defects in the cuticle (*dpy-9* and *dpy-10*) and that express innate immune genes including *nlp-29* constitutively at a high level[19,26]. The high expression of *nlp-29p::gfp* in both mutants was reduced upon *dcar-1(RNAi)* (Fig 3a).

As measured by qRT-PCR, the expression of all 6 genes of the *nlp-29* locus was increased in a *dpy-10* mutant background, to varying degrees (Fig. 3b). Loss of *dcar-1* function reduced this elevated expression of the *nlp-29* locus genes (Fig. 3c), by 60–90% for *nlp-27*, *nlp-30*, *nlp-31* and *nlp-34* and by 20–40% for *nlp-28* and *nlp-29* (Fig. 2c). The two genes that show the smallest relative change in expression and least *dcar-1*-dependency in the *dpy-10* background (*nlp-28* and *nlp-29*) are those that exhibit the greatest comparative *pmk-1*-independent increase in expression upon osmotic stress[19]. These results suggest that the elevated expression of *nlp* genes in the *dpy-10* mutant background likely has 2 causes, the intrinsic alteration of osmotic homeostatic mechanisms that characterizes a subset of Dpy mutants[26,27] and the alteration of the structural integrity of the cuticle observed in Dpy mutants[28], which may be perceived as a wound. This supports the idea that an endogenous ligand generated when the integrity of the epidermis and/or cuticle is compromised, acting through *dcar-1* and the p38 MAPK cascade, triggers AMP gene expression.

## DCAR-1 acts cell-autonomously in the epidermis

Examination of strains carrying a rescuing translational reporter gene (*dcar-1p::dcar-1::gfp*; see below) revealed that *dcar-1* was expressed on the apical surface in the major epidermal syncytium, hyp7 (Fig. 4a), and confirmed its previously described neuronal expression

Author Manuscript Author Manuscript Author Manuscript Author Manuscript

domain[25] (in the neurons called ASH, ASI and PVQ; data not shown). In neurons, *dcar-1* mediates an avoidance response to specific repellents, acting in concert with *ocr-2* and *osm-9*[25]. Unlike RNAi against *dcar-1*, RNAi against these 2 genes had no effect on *nlp-29p::gfp* expression (Supplementary Fig. 2a). Knocking down *dcar-1* expression specifically in the adult epidermis, the site of expression of the infection-inducible *nlp* genes, greatly decreased *nlp-29p::gfp* expression upon infection (Supplementary Fig. 2b). Conversely, expressing *dcar-1::gfp* under the control of the *dcar-1* promoter, or specifically in the epidermis using the *col-12* promoter, led to a restoration of AMP gene expression after *D. coniospora* infection, and was associated with rescue of the mutant's resistance to infection. Expressing *dcar-1* only in the neurons ASH, ASI and PVQ, using the *sra-6* promoter, rescues the *dcar-1* mutant's avoidance phenotype[25], but was not associated with any rescue of AMP expression or resistance (Fig. 4b,c; Supplementary Fig. 3). Together, these results clearly demonstrate that *dcar-1* acts in an epidermis-specific and cell-autonomous manner to regulate AMP gene expression and defense against infection, and this via a pathway that differs from that involved in its neuronal function.

## Dihydrocaffeic acid can activate DCAR-1 in the epidermis

Dihydrocaffeic acid (DHCA) has been described as a potent ligand for DCAR-1 in both *in vivo* and in heterologous *Xenopus* oocyte assays[25]. We found that direct addition of DHCA to wild-type worms triggered *nlp-29p::gfp* reporter gene expression in a dose-dependent manner. This increase was absent in *dcar-1* mutant worms and mutants for several elements of the regulatory network that controls *nlp-29* gene expression (Fig. 5a,b). DHCA exposure also triggered an increase in the expression of all 6 *nlp* genes from the *nlp-29* cluster within 2 hours that was largely *dcar-1* and *pmk-1* dependent (Fig. 5c and Supplementary Fig. 4a). Expression of *dcar-1* in the epidermis, but not in neurons, was sufficient to restore the induction of the different *nlp* genes by DHCA (Fig. 5c). DHCA did not, however, trigger any *dcar-1*-dependent variation in the expression of several candidate intestinal defense genes (Supplementary Fig. 4b,c). Together, these results show that DHCA can act as an exogenous ligand that activates the innate immune response in the nematode epidermis via DCAR-1.

## Identification of an *in vivo* ligand for DCAR-1

A number of molecules that are structurally related to DHCA also activate DCAR-1[25]. We therefore tested them as well as 3,4-dihydroxyphenylalanine DOPA, the DOPA derivative 3-(3,4-dihydroxy-phenyl)pyruvate (DPPA), tyrosine, the tyrosine derivative 4-hydroxyphenyllactic acid (HPLA) and several others. Of the 13 compounds tested, only 4, 3-(2 4-dihydroxyphenyl)propionic acid (DHPA), DHCA, DPPA and HPLA triggered *nlp-29p::gfp* reporter gene expression in a dose-dependent manner, with all 4 molecules having comparable effects (Fig. 6a; Supplementary Fig. 5).

To determine if any of the 4 active compounds might correspond to the *in vivo* ligand for DCAR-1, we undertook a direct biochemical approach, analyzing extracts from control and infected worms via mass spectrometry-based comparative metabolomics. Whereas DHPA, DPPA, and DHCA were not detected, these analyses revealed that HPLA was present at a low level in control worms, and increased upon infection (Fig. 6b). The amount of HPLA

Author Manuscript Author Manuscript Author Manuscript Author Manuscript

was also elevated in *dpy-10* mutants, both in extracts from pellets of worms and from the culture medium when worms were grown in liquid (Fig. 6b,c). This confirms that as well as being produced upon infection, HPLA can be generated in the absence of infection as a consequence of alterations of the cuticle. We observed a robust time-dependent increase in HPLA levels upon infection (Fig. 7a). The increase in *nlp-29p::gfp* expression provoked by addition of HPLA was dependent upon *dcar-1* and multiple elements of the downstream signal transduction cascade (Fig. 7b). These results indicate that HPLA can act through DCAR-1 to regulate the epidermal innate immune response.

Although its biosynthetic pathway has not been characterized in any eukaryote, HPLA is likely derived from tyrosine, for example through the action of an aminotransferase and subsequent reduction of 4-hydroxyphenylpyruvate (Supplementary Fig. 6a). While knocking down the expression of individual candidate aminotransferases in the epidermis had no detectable effect on *nlp-29p::gfp* expression after infection, possibly due to functional redundancy (Supplementary Fig. 6b), overexpressing the candidate aminotransferase *tatn-1*[29] in the adult epidermis led to the predicted increase in *nlp-29p::gfp* expression after infection, which was *dcar-1*-dependent (Fig. 7c). This provides further support for HPLA being an endogenous signal, or damage-associated molecular pattern (DAMP), that triggers the up-regulation of defense genes via the GPCR DCAR-1 in the epidermis (Supplementary Fig. 7).

## DISCUSSION

In this study, we demonstrated that DCAR-1 is specifically required for the innate immune response to fungal infection and wounding and place this GPCR further upstream than any other known component of innate immune recognition and signaling in *C. elegans* epidermis. Since it appears to play a role in DAMP recognition, DCAR-1 may be important for regulating the response to a variety of different pathogens if they cause cellular damage like *D. coniospora*. It is interesting to note that strains of *Leucobacter* induce damage and *nlp-29* expression[30,31]. This induction of AMP gene expression would be predicted to be blocked in a *dcar-1* mutant. Clear homologs of DCAR-1 can be found in nematode genomes, but not in other animals'. It could be that receptor(s) for HPLA exist outside the nematode phylum, but are not recognizable from their primary sequence. Alternatively, the use of a receptor for HPLA as a DAMP receptor may be specific to nematodes, possibly reflecting some unique aspect of their physiology or anatomy. It should be noted, however, that HPLA is a common tyrosine metabolite and can be detected across species, including in humans. Its level is elevated in patients with a deficiency of p-hydroxyphenylpyruvate oxidase[32], and with Zellweger's syndrome[33], but a specific link between HPLA and innate immunity has yet to be established in any other species.

The GPCR family is greatly expanded in *C. elegans*[34]. Members show considerable genetic diversity, with evidence for positive selection in some. This has been hypothesized to reflect a role in pathogen recognition[35,36]. DCAR-1 may thus be one of several GPCRs involved in mediating host-pathogen responses in *C. elegans*. It is not known whether any GPCR recognizes specific microbe-associated molecular patterns.

Author Manuscript Author Manuscript Author Manuscript Author Manuscript

Recently, uracil was found to provoke intestinal inflammation in *Drosophila*, via an as yet unidentified GPCR[6], while specific taste receptor GPCRs in the mammalian nose detect bacterially-derived signals and can regulate upper respiratory innate immunity in mice and humans[7–9]. Our finding that ligand-activated DCAR-1 is required for immune defenses against *D. coniospora* reinforces the notion that GPCRs constitute an important, but largely unexplored conserved class of immuno-modulatory receptors in many species.

Activation of DCAR-1 in the epidermis regulates immune defenses. Neuronally-expressed DCAR-1 has been shown to play a role in aversive behavior[25], which can protect *C. elegans* from pathogen exposure[10,37]. So DCAR-1 potentially has a second role in host defense. The strength of the repulsion phenotype that worms display in the presence of certain pathogens is dependent on the density of the worm population, possibly reflecting inter-organism signaling[38]. It is interesting to speculate that DCAR-1 could be involved.

We provide strong correlative evidence that HPLA is an endogenous ligand for DCAR-1. Proving this definitively is not straightforward since to manipulate HPLA levels involves altering tyrosine metabolism, which can affect many aspects of worm development and physiology[29], including the formation of the cuticle[39] and thus influence *nlp* gene expression in multiple ways. Nevertheless, understanding the mechanisms leading to the observed infection-dependent increase in HPLA will be of great interest. One open question is whether *D. coniospora* contributes actively to HPLA production, or whether the increase in HPLA is purely a consequence of host mechanisms brought into play by the physical disruption of the cuticle and/or epidermis that occurs as the infection progresses[17]. In either case, HPLA appears to act as a DAMP, to the best of our knowledge, the first described for *C. elegans*.

## ONLINE METHODS

### Nematode strains

All strains were maintained on nematode growth media (NGM) and fed with *E. coli* strain OP50. The wild-type reference strain is N2 Bristol. The strains *dcar-1(nj66)* and *dcar-1(tm2484)*[1] were kindly provided by Y. Goshima, *tir-1(tm3036)* by S. Mitani, *pmk-1(km25)* and *gpa-12(pk322)* were obtained from the *Caenorhabditis* Genetics Center (CGC) and *tpa-1(fr1)* described elsewhere[2]. Details about the strains IG274 (containing *frIs7*[*nlp-29p::gfp*, *col-12p::DsRed*] *IV*) and IG1389 (containing *frIs7* and *frIs30*[*col-19p::gpa-12**,*unc-53pB::gfp*] *I*) are given elsewhere[3,4]. The screening of GPCR genes by RNAi was performed in 96-well plates as described[5]. All other RNAi feeding experiments were performed essentially as described[2].

### RNA interference

For the genome-wide screen, clones were used directly from the Ahringer[6] and the Vidal[7] RNAi libraries. For subsequent studies, insert sequences were verified before use. The clone targeting *tpa-1* was described previously[2].

Author Manuscript Author Manuscript Author Manuscript Author Manuscript

For epidermal-specific RNAi, the *frIs7[nlp-29p::gfp, col-12p::DsRed]* transgene was crossed into two strains CZ14540 *rde-1(ne219) V; juls346[col-19p::RDE-1]*[8] and JM43 *rde-1(ne219); Is[wrt-2p::rde-1; myo-2p::rfp]*[9].

## Constructs and transgenic lines

All the mutant strains carrying frIs7[nlp-29p::gfp, col-12p::DsRed] or frIs30[col-19p::gpa-*12***,pNP21(unc-53pB::gfp)]* were obtained by conventional crosses with the IG274[3] and IG1389[4] strains, respectively. Full genotypes of the transgenic strains are given below. The *dcar-1p::dcar-1::gfp* construct contains 2.5 kilobases of genomic sequence upstream of the start codon of C06H5.7 and was obtained by PCR fusion as described[10] using PCR fusion primers JEP2018, JEP2019; JEP2020, JEP2117, JEP2048, JEP2120, JEP568, JEP572, JEP2120, JEP569 and JEP570 using *dcar-1* cDNA[1], the kind gift of Y. Goshima, and the vector pPD95.75 as templates. Microinjections were performed using 20 ng/μl of the construct and the coinjection marker *col-12p::DsRed*[3] or pRF4[*rol-6(su1006)*] at a concentration of 80 ng/μl into *dcar-1*(*tm2484*) animals. From six independent lines generated, IG1473 and IG1476 were retained for further study.

To drive expression of *dcar-1::gfp* specifically in the epidermis a *col-12p::dcar-1::gfp* construct was generated by PCR fusions using PCR fusion primers: JEP367, JEP568, JEP569, JEP572, JEP902, JEP2047, JEP2048, JEP2120, JEP368 and JEP570 using *dcar-1* cDNA[1], and the vectors *col-12p::DsRed*[3] and pPD95.75 as templates. A second construct, *col-12p::dcar-1*, was also generated using PCR fusion primers JEP902, JEP368, JEP2047, JEP2048, JEP2049, JEP2051 using the vector *col-12p::DsRed*[3] and *dcar-1* cDNA[1] as templates. The *sra-6p::dcar-1::Venus* and *sra-6p::dcar-1* plasmids[1] for specific neuronal expression of *dcar-1* were generous gifts of Y. Goshima. Microinjections were performed using 20 ng/μl of the construct of interest and the coinjection marker *col-12p::DsRed*[3] or pNP21[*unc-53pB::gfp*][11] at a concentration of 80 ng/μl in *dcar-1(tm2487)* or IG1424 *dcar-1(tm2484); frIs7* strains. Several lines for each construct were obtained. The lines IG1479, IG1482, IG1435 and IG1438 were retained for further study.

The *col-19p::tatn-1*construct was generated by Gibson cloning, fusing the promoter of *col-19* amplified from the vector pCZGY1434 kindly provided by A. Chisholm[8] using primers JEP2244 and JEP2245, with the *tatn-1* gene including its 3′UTR with the primers JEP2246 and JEP2247.

The construct was injected at 5 ng/μl together with pNP21[*unc-53pB::gfp*][11] at 80 ng/ml in IG274. Two lines were generated IG1523 and IG1524 that gave equivalent results in initial characterization. The strain IG1523 was retained for further study. The level of *tatn-1* expression was determined by qRT-PCR from two independent experiments to be 3.1-fold higher (+/−0.5) in the samples from this strain that from age-matched wild-type worms (average and SD).

## PCR fusion and Gibson primers

The sequences of the primers used are:

JEP2019: cataggatgcgcacaattatgtcg,

Author Manuscript Author Manuscript Author Manuscript Author Manuscript

JEP2018: aggtcttaagttcgaactccgc,

JEP2020: atcggaacatgcggcattgca,

JEP902: cagtctatgcgttaaaaatc,

JEP367: catgcatgcacggccaggaacggagcc,

JEP368: tcagtatttgctattgac,

JEP2047: ctgtacgttggtttgcactcatttttctaaaaagtaatca,

JEP2048: atgagtgcaaaccaacgtacag,

JEP2049: cacacaggaaacagctatgacc,

JEP2051: taattagaatcgttcaaccttccgatcaac,

JEP2117: ctgtacgttggtttgcactcatgtcatctgaataaagattatgtattg,

JEP2120: agtcgacctgcaggcatgcaagctgaatcgttcaaccttccgatcaac,

JEP568: agcttgcatgcctgcaggtcgact,

JEP569: aagggcccgtacggccgactagtagg,

JEP570: ggaaacagttatgtttggtatattggg,

JEP572: aaacgcgcgagacgaaag,

JEP2244: gaaagacatcagttcatcaacatgcaaactctaatgagtcac,

JEP2245: caattaaccctcactaaaggattttgctggattcaatgcg,

JEP2246: cctttagtgagggttaattg,

JEP2247: gttgatgaactgatgtctttc.

## Chemicals

Tyrosine, 3-4-hydroxy-phenyl-propionic acid (HPA), 3,4-dihydrobenzaldehyde (DHB), 3,4-dihyroxybenzoic acid (DHBA), 3,4 dihydroxymandelic acid (DHMA), L-3,4-dihydroxyphenylalanine (DOPA) and 3,4-dihydroxyphenylacetic acid (DOPAC), 3,4-hydroxyphenyl lactic acid (HPLA), 2,4-Dihydroxyphenyl propionic acid (DHPA) and 4-hydroxyphenylpyruvic acid (HPPA) were purchased from Sigma-Aldrich; dihydrocaffeic acid (DHCA), 3,4-dihydroxy-phenyl pyruvate (DPPA) and 3-4-dihydroxyphenyl lactic acid (DPLA) were obtained from Extrasynthese, Molekula and Stanford Chemicals respectively. With the exception of DOPA, stock solutions at 1M were prepared in 70% ethanol, aliquoted and stored at −20°C. For subsequent dilution to a final concentration below 20 mM, fresh aliquots were first diluted to 50 mM in deionized water and then to their final concentration in 50 mM NaCl. For DOPA, a 10 mM stock solution was prepared in 50 mM NaCl, aliquoted and stored at −20°C. Fresh aliquots were diluted to their final concentration in 50 mM NaCl.

Author Manuscript Author Manuscript Author Manuscript Author Manuscript

### Infection, wounding osmotic stress and PMA treatment

Infections, epidermal wounding, PMA treatment and osmotic stress were performed as previously described[2].

### Killing assays

50–70 worms at the young adult stage were infected at 20°C for 16 h with *D. coniospora* then transferred to fresh plates and the surviving worms were counted every day as described elsewhere[12]. Assays with *P. aeruginosa* strain PA14 and *E. coli* strain OP50 used 70–100 worms at the young adult stage and were done at 25°C using full-plate lawns as described[13]. In contrast to PA14 that repels *C. elegans*, spores of *D. coniospora* attract worms[14]. For assays with *D. coniospora*, standard OP50 plates were used. Spores were spread uniformly across the bacterial lawn. There was no obvious difference in lawn occupancy between wild-type and other strains. Statistical analyses used one-sided log rank test within Prism (Graphpad software).

### Analyses with the Biosort worm sorter

Expression of *nlp-29p::gfp* and *dcar-1p::gfp* reporters was quantified with the COPAS Biosort (Union Biometrica). Generally a minimum of 80 synchronized worms were analyzed for size (TOF), extinction (EXT), green (GFP) and red (dsRed) fluorescence[15]. The ratio Green/Red was then calculated to correct for variations in size and health of individual worms and potential non-specific effects on transgene expression[3]. In one case where the red fluorescence was markedly different between populations of worms (Fig. 3a), the Green/TOF ratio was used. When only mean values for ratios are presented, the values for the different samples within a single experiment are normalized so that the control worms (generally WT) had a fluorescence ratio of 1. As discussed more extensively elsewhere[3], as the distribution of fluorescence ratios is far from normal, standard deviations are not an appropriate parameter and are not shown on figures with the Biosort. The results shown are representative of at least 3 independent biological replicates.

### RNA preparation and quantitative RT -PCR

RNA preparation and quantitative RT-PCR were done as described[3]. Results were normalized to those of *act-1* and were analyzed by the cycling threshold method. Control and experimental conditions were tested in the same ‘run’. Each sample was normalized to its own *act-1* control to take into account age-specific changes in gene expression.

### qRT-PCR primers

Primers used for qRT-PCR are for:

*act-1:* JEP538 ccatcatgaagtgcgacattg JEP539 catggttgatggggcaagag;

*dcar-1:* JEP2030 cctacgctatttggtgcattggct JEP2031 tgcaccgaatcaccagaaacag;

*nlp-27:* JE965 cggtggaatgccatatggtg JEP966 atcgaatttactttccccatcc;

*nlp-28:* JEP967 tatggaagaggttatggtgg JEP968 gctaatttgtctactttcccc;

*nlp-29:* JEP952 tatggaagaggatatggaggatatg JEP848 tccatgtatttactttccccatcc;

Author Manuscript Author Manuscript Author Manuscript Author Manuscript

*nlp-30:* JEP948 tatggaagaggatatggtggatac JEP949 ctactttccccatccgtatcc;

*nlp-31:* JEP950 ggtggatatggaagaggttatggag JEP953 gtctatgcttttactttcccc;

*nlp-34:* JEP969 atatggataccgcccgtacg JEP970 ctattttccccatccgtatcc;

*pgp-5:* JEP558 ggaaaatcagaatgggacga JEP559 ttgattgccatgaatggtgt;

*irg-1:* JEP1676 ccatggaatgaaacttgtgg JEP1677 ccagtttcgttcatcttcaca;

*irg-3:* JEP1678 tcgatcaatgtgatgctcag JEP1678 ccgcctgacagttgaagtc;

*F49F1.6:* JEP1680 ccatcaactacgccaaagc JEP1681 tccggtggatagaaggtgtt;

*F57F4.4:* JEP1910 gtacctccttgaacttgaccaactcg JEP1911 gtgtggttacaattcctgggcc;

*tatn-1:* JEP2260 tcttgagcaagccaaaccgc JEP2261 aggtacggcgcaagcatcag.

## Identification of GPCR genes

WormMart (WS220) was queried using a broad set of GPCR domain denominations derived from InterPro 37.0 (http://www.ebi.ac.uk/interpro/): IPR000162, IPR000276, IPR000337, IPR000344, IPR000405, IPR000609, IPR000611, IPR000832, IPR000995, IPR001402, IPR001817, IPR001879, IPR002002, IPR002131, IPR002184, IPR002231, IPR002455, IPR002456, IPR003839, IPR004151, IPR005047, IPR009126, IPR009144, IPR011500, IPR015672, IPR017978, IPR017979, IPR017983, IPR018817, IPR019336, IPR019408, IPR019420, IPR019421, IPR019422, IPR019423, IPR019424, IPR019425, IPR019426, IPR019427, IPR019428, IPR019429, IPR019430.

## Preparation of worm pellet and supernatant extracts for high-resolution HPLC-MS analysis

10 ml of packed worm pellets from flash-frozen samples of *C. elegans* wild-type control, infected (4, 5, 6, and 7 h post-infection), and *dpy-10* animals were lyophilized and crushed in a mortar-pestle over granular dry ice to a fine powder. The powders were extracted with 25 ml of ethanol for 14 h and filtered. The extracts were concentrated *in vacuo*, resuspended in 250 μL methanol, filtered, and 2 μL used for HPLC-MS runs without further processing. *dpy-10* worms were additionally grown in 100 mL liquid culture and the culture supernatant processed as previously reported[16]. The resulting supernatant extract was resuspended in 750 μL methanol, filtered, and 2 μL used for HPLC-MS runs without further processing.

## High-resolution HPLC-MS instrumentation, conditions, and analyses

High-resolution HPLC-MS was performed using a Waters nanoACQUITY UPLC system using a Waters Acquity UPLC HSS C-18 column (2.1 × 100 mm, 1.8 μm particle diameter) connected to a Xevo G2 QTof mass spectrometer operated in electrospray negative (ESI-) ionization mode. A 0.1% formic acid in water (aqueous) − 0.1% formic acid in acetonitrile (organic) solvent system was used at a flow rate of 0.5 mL/min, starting with the organic solvent content of 5% for 2 min and increasing to 100% over a period of 14 min. Worm pellet and supernatant extracts were analyzed by HPLC-ESI-MS in negative mode using a capillary voltage of 3.1 kV and a cone voltage of −30 V with the MS operating in scanning mode for a mass range of *m/z* 100–700.

Author Manuscript Author Manuscript Author Manuscript Author Manuscript

The resulting high-resolution HPLC-MS data from the different extracts were analyzed using Waters MassLynx™ 4.1 software to identify compounds with a different abundance in samples from infected and *dpy-10* worms as compared to the control. The most prominent difference was observed for a compound eluting at around 4.28 min with a high-resolution mass corresponding to the molecular ion for a dihydroxy phenylpropionic acid derivative, such as HPLA or DHCA. Comparison of the retention time of this dihydroxy phenylpropionic acid with that of synthetic HPLA and DHCA showed that it precisely matched that of synthetic HPLA, which is distinctly different from that of DHCA (Fig. 6b). To conclusively assign the observed dihydroxy phenylpropionic acid as HPLA and confirm the absence of DHCA, a mixing experiment was conducted wherein the *dpy-10* supernatant extract was spiked with synthetic HPLA and DHCA and the corresponding high resolution HPLC-MS analyzed. Upon mixing, the relative intensity of the HPLA peak increased and a new peak for DHCA appeared in the chromatogram. An unrelated peak, which corresponds to an as-yet unidentified compound in the supernatant extract, eluting at 5 minutes, was also observed. This compound was not detected in samples from control or infected wild-type worms, and only in trace quantities in samples extracted from whole *dpy-10* worms. With the increase in the HPLA and DHCA peaks, it shows a corresponding decrease in relative intensity in the mixed sample (Fig. 6c). To compare the abundance of HPLA in *C. elegans* wild-type control and infected samples (as in Fig. 7a), the corresponding HPLC-MS peak integrations (ESI-, ion chromatogram for *m/z* = 181), normalized by the worm pellet dry weight obtained for each condition were used.

## Full genotypes of transgenic strains

IG274 WT*; frIs7[nlp-29p::gfp, col-12p::DsRed] IV*$^{3}$

IG1389 WT; *frIs7 IV; frIs30[col-19p::gpa-12*,pNP21(unc-53pB::gfp)] I*$^{4}$

IG460 *pmk-1(km25) frIs7 IV*$^{3}$

IG692 *tir-1(tm3036) III; frIs7 IV*$^{3}$

IG722 *gpa-12(pk322) X; frIs7 IV*$^{2}$

IG293 *tpa-1(fr1) frIs7 IV*$^{2}$

IG466 *dpy-9(e12) frIs7 IV*$^{17}$

IG1327 *rde-1(ne219) V; juls346[col-19p::rde-1] III; frIs7 IV*

IG1502 *rde-1(ne219) V; Is[wrt-2p::rde-1; myo-2p::rfp]; frIs7 IV*

IG1457 *dpy-10(e128) II; frIs7 IV*

IG1424 *dcar-1(tm2484) V; frIs7 IV*

IG1473 *dcar-1(tm2484) V; frEx535[dcar-1p::dcar-1::gfp,pRF4(rol-6(su1006)]*

IG1474 *dcar-1(tm2484) V; frEx536[dcar-1p::dcar-1::gfp,pRF4(rol-6(su1006)]*

IG1475 *dcar-1(tm2484) V; frEx537[dcar-1p::dcar-1::gfp,pRF4(rol-6(su1006)]*

IG1476 *dcar-1(tm2484) V; frEx538[dcar-1p::dcar-1::gfp,col-12p::DsRed]*

Author Manuscript Author Manuscript Author Manuscript Author Manuscript

IG1477 *dcar-1(tm2484) V; frEx539[dcar-1p::dcar-1::gfp,col-12p::DsRed]*

IG1478 *dcar-1(tm2484) V; frEx540[dcar-1p::dcar-1::gfp,col-12p::DsRed]*

IG1479 *dcar-1(tm2484) V; frEx541[col-12p::dcar-1::gfp, col-12p::DsRed]*

IG1482 *dcar-1(tm2484) V; frEx544[sra-6p::dcar-1::Venus, col-12p::DsRed]*

IG1435 *dcar-1(tm2484) V; frIs7 IV; frEx514[sra-6p::dcar-1, pNP21(unc-53pB::gfp)]*

IG1438 *dcar-1(tm2484) V; frIs7 IV; frEx517[col-12p::dcar-1, pNP21(unc-53pB::gfp)]*

IG1523 WT*; frIs7 IV; frEx564[col-19p::tatn-1, pNP21(unc-53pB::gfp)]*

IG1524 WT*; frIs7 IV; frEx565[col-19p::tatn-1, pNP21(unc-53pB::gfp)]*

## Supplementary Material

Refer to Web version on PubMed Central for supplementary material.

## Acknowledgments

We thank A. Chisholm and Y. Goshima for strains and reagents, C. Bargmann, A. Chisholm, C. Couillault, P. Golstein and E. Vivier for critical reading of the manuscript, M. Metwaly, F. Montañana Sanchis, S. Omi, J. Soulé and the staff at Wormbase and ModulBio for technical support, C. Melon for advice. Some nematode strains were provided by the CGC, which is funded by NIH Office of Research Infrastructure Programs (P40 OD010440), or by the National Bioresource Project coordinated by S. Mitani. This work was funded by institutional grants from INSERM and CNRS, program grants from the PACA Regional Council, the ANR (MIME-2007 and ANR-12-BSV3-0001-01 to JJE), and the NIH (GM088290 to FCS). BS was supported in part by the Fondation ARC.

## References

1. Ausubel FM. Are innate immune signaling pathways in plants and animals conserved? Nat Immunol. 2005; 6:973–979. [PubMed: 16177805]
2. Mallo GV, et al. Inducible antibacterial defense system in *C. elegans*. Curr Biol. 2002; 12:1209–1214. [PubMed: 12176330]
3. Kim DH, et al. A conserved p38 MAP kinase pathway in *Caenorhabditis elegans* innate immunity. Science. 2002; 297:623–626. [PubMed: 12142542]
4. Visvikis O, et al. Innate Host Defense Requires TFEB-Mediated Transcription of Cytoprotective and Antimicrobial Genes. Immunity. 2014; 40:896–909.10.1016/j.immuni.2014.05.002 [PubMed: 24882217]
5. Shapira M, et al. A conserved role for a GATA transcription factor in regulating epithelial innate immune responses. Proc Natl Acad Sci U S A. 2006; 103:14086–14091. [PubMed: 16968778]
6. Lee KA, et al. Bacterial-derived uracil as a modulator of mucosal immunity and gut-microbe homeostasis in *Drosophila*. Cell. 2013; 153:797–811.10.1016/j.cell.2013.04.009 [PubMed: 23663779]
7. Saunders CJ, Christensen M, Finger TE, Tizzano M. Cholinergic neurotransmission links solitary chemosensory cells to nasal inflammation. P Natl Acad Sci USA. 2014; 111:6075–6080.10.1073/pnas.1402251111
8. Tizzano M, et al. Nasal chemosensory cells use bitter taste signaling to detect irritants and bacterial signals. P Natl Acad Sci USA. 2010; 107:3210–3215.10.1073/pnas.0911934107
9. Lee RJ, et al. Bitter and sweet taste receptors regulate human upper respiratory innate immunity. J Clin Invest. 2014; 124:1393–1405.10.1172/JCI72094 [PubMed: 24531552]
10. Reddy KC, Andersen EC, Kruglyak L, Kim DH. A polymorphism in *npr-1* is a behavioral determinant of pathogen susceptibility in *C. elegans*. Science. 2009; 323:382–384. [PubMed: 19150845]

Author Manuscript Author Manuscript Author Manuscript Author Manuscript


11. Powell JR, Kim DH, Ausubel FM. The G protein-coupled receptor FSHR-1 is required for the *Caenorhabditis elegans* innate immune response. Proc Natl Acad Sci U S A. 2009; 106:2782–2787. [PubMed: 19196974]
12. McEwan DL, Kirienko NV, Ausubel FM. Host translational inhibition by *Pseudomonas aeruginosa* Exotoxin A Triggers an immune response in *Caenorhabditis elegans*. Cell Host Microbe. 2012; 11:364–374. S1931–3128(12)00091–1 [pii]. 10.1016/j.chom.2012.02.007 [PubMed: 22520464]
13. Melo JA, Ruvkun G. Inactivation of conserved *C.elegans* genes engages pathogen- and xenobiotic-associated defenses. Cell. 2012; 149:452–466. S0092-8674(12)00346-7 [pii]. 10.1016/j.cell.2012.02.050 [PubMed: 22500807]
14. Dunbar TL, Yan Z, Balla KM, Smelkinson MG, Troemel ER. *C.elegan*s detects pathogen-induced translational inhibition to activate immune signaling. Cell Host Microbe. 2012; 11:375–386. S1931-3128(12)00092-3 [pii]. 10.1016/j.chom.2012.02.008 [PubMed: 22520465]
15. Partridge FA, Gravato-Nobre MJ, Hodgkin J. Signal transduction pathways that function in both development and innate immunity. Developmental dynamics. 2010; 239:1330–1336.10.1002/dvdy.22232 [PubMed: 20131356]
16. Pukkila-Worley R, Ausubel FM. Immune defense mechanisms in the *Caenorhabditis elegans* intestinal epithelium. Current opinion in immunology. 2012; 24:3–9.10.1016/j.coi.2011.10.004 [PubMed: 22236697]
17. Dijksterhuis J, Veenhuis M, Harder W. Ultrastructural study of adhesion and initial stages of infection of the nematode by conidia of *Drechmeria coniospora*. Mycological research. 1990; 94:1–8.
18. Couillault C, et al. TLR-independent control of innate immunity in *Caenorhabditis elegans* by the TIR domain adaptor protein TIR-1, an ortholog of human SARM. Nat Immunol. 2004; 5:488–494. [PubMed: 15048112]
19. Pujol N, et al. Anti-fungal innate immunity in *C.elegans* is enhanced by evolutionary diversification of antimicrobial peptides. PLoS Pathog. 2008; 4:e1000105.10.1371/journal.ppat.1000105 [PubMed: 18636113]
20. Pujol N, et al. Distinct innate immune responses to infection and wounding in the *C.elegans* epidermis. Curr Biol. 2008; 18:481–489. S0960-9822(08)00361-8 [pii]. 10.1016/j.cub.2008.02.079 [PubMed: 18394898]
21. Dierking K, et al. Unusual regulation of a STAT protein by an SLC6 family transporter in *C.elegans* epidermal innate immunity. Cell Host Microbe. 2011; 9:425–435. S1931-3128(11)00133-8 [pii]. 10.1016/j.chom.2011.04.011 [PubMed: 21575913]
22. Ziegler K, et al. Antifungal innate immunity in *C.elegans*: PKCdelta links G protein signaling and a conserved p38 MAPK cascade. Cell Host Microbe. 2009; 5:341–352. S1931-3128(09)00097-3 [pii]. 10.1016/j.chom.2009.03.006 [PubMed: 19380113]
23. Squiban B, Belougne J, Ewbank J, Zugasti O. Quantitative and automated high-throughput genome-wide RNAi screens in *C.elegans*. J Vis Exp. 2012; 60:e3448.10.3791/3448
24. Labed SA, Omi S, Gut M, Ewbank JJ, Pujol N. The pseudokinase NIPI-4 is a novel regulator of antimicrobial peptide gene expression. PLoS One. 2012; 7:e33887. PONE-D-12-00698 [pii]. 10.1371/journal.pone.0033887 [PubMed: 22470487]
25. Aoki R, et al. A seven-transmembrane receptor that mediates avoidance response to dihydrocaffeic acid, a water-soluble repellent in *Caenorhabditis elegans*. J Neurosci. 2011; 31:16603–16610.10.1523/JNEUROSCI.4018-11.2011 [PubMed: 22090488]
26. Rohlfing AK, Miteva Y, Hannenhalli S, Lamitina T. Genetic and physiological activation of osmosensitive gene expression mimics transcriptional signatures of pathogen infection in *C. elegans*. PLoS One. 2010; 5:e9010. [PubMed: 20126308]
27. Wheeler JM, Thomas JH. Identification of a novel gene family involved in osmotic stress response in *Caenorhabditis elegans*. Genetics. 2006
28. Cox GN, Laufer JS, Kusch M, Edgar RS. Genetic and Phenotypic Characterization of Roller Mutants of *Caenorhabditis elegans*. Genetics. 1980; 95:317–339. [PubMed: 17249038]

Author Manuscript Author Manuscript Author Manuscript Author Manuscript

29. Ferguson AA, et al. TATN-1 mutations reveal a novel role for tyrosine as a metabolic signal that influences developmental decisions and longevity in *Caenorhabditis elegans*. PLoS Genet. 2013; 9:e1004020.10.1371/journal.pgen.1004020 [PubMed: 24385923]

30. Muir RE, Tan MW. Virulence of *Leucobacter chromiireducens* subsp.*solipictus* to *Caenorhabditis elegans*: characterization of a novel host-pathogen interaction. Appl Environ Microbiol. 2008; 74:4185–4198. AEM.00381-08 [pii]. 10.1128/AEM.00381-08 [PubMed: 18487405]

31. Hodgkin J, Felix MA, Clark LC, Stroud D, Gravato-Nobre MJ. Two *Leucobacter* strains exert complementary virulence on *Caenorhabditis* including death by worm-star formation. Current biology : CB. 2013; 23:2157–2161.10.1016/j.cub.2013.08.060 [PubMed: 24206844]

32. Mrochek JE, Dinsmore SR, Ohrt DW. Monitoring phenylalanine-tyrosine metabolism by high-resolution liquid chromatography of urine. Clin Chem. 1973; 19:927–936. [PubMed: 4720815]

33. Mayatepek E, Seppel CK, Hoffmann GF. Increased urinary excretion of dicarboxylic acids and 4-hydroxyphenyllactic acid in patients with Zellweger syndrome. Eur J Pediatr. 1995; 154:755–756. [PubMed: 8582432]

34. Bargmann, CI. The *C. elegans* Research Community, editor. WormBook. 2006. p. 1-29.http://www.wormbook.org

35. Stewart MK, Clark NL, Merrihew G, Galloway EM, Thomas JH. High genetic diversity in the chemoreceptor superfamily of *Caenorhabditis elegans*. Genetics. 2005; 169:1985–1996. [PubMed: 15520260]

36. Thomas JH, Kelley JL, Robertson HM, Ly K, Swanson WJ. Adaptive evolution in the SRZ chemoreceptor families of *Caenorhabditis elegans* and *Caenorhabditis briggsae*. Proc Natl Acad Sci U S A. 2005; 102:4476–4481. [PubMed: 15761060]

37. Pradel E, et al. Detection and avoidance of a natural product from the pathogenic bacterium *Serratia marcescens* by *Caenorhabditis elegans*. Proc Natl Acad Sci U S A. 2007; 104:2295–2300. [PubMed: 17267603]

38. Pujol, N.; Ewbank, JJ. Toll Receptors. Rich, T., editor. Vol. Ch 7. Landes Bioscience Press; 2003.

39. Kim TH, Hwang SB, Jeong PY, Lee J, Cho JW. Requirement of tyrosylprotein sulfotransferase-A for proper cuticle formation in the nematode *C.elegans*. FEBS Lett. 2005; 579:53–58.10.1016/j.febslet.2004.11.044 [PubMed: 15620690]

## REFERENCES

1. Aoki R, et al. A seven-transmembrane receptor that mediates avoidance response to dihydrocaffeic acid, a water-soluble repellent in *Caenorhabditis elegans*. J Neurosci. 2011; 31:16603–16610.10.1523/JNEUROSCI.4018-11.2011 [PubMed: 22090488]

2. Ziegler K, et al. Antifungal innate immunity in *C. elegans*: PKCdelta links G protein signaling and a conserved p38 MAPK cascade. Cell Host Microbe. 2009; 5:341–352. S1931-3128(09)00097-3 [pii]. 10.1016/j.chom.2009.03.006 [PubMed: 19380113]

3. Pujol N, et al. Distinct innate immune responses to infection and wounding in the *C. elegans* epidermis. Curr Biol. 2008; 18:481–489. S0960-9822(08)00361-8 [pii]. 10.1016/j.cub.2008.02.079 [PubMed: 18394898]

4. Labed SA, Omi S, Gut M, Ewbank JJ, Pujol N. The pseudokinase NIPI-4 is a novel regulator of antimicrobial peptide gene expression. PLoS One. 2012; 7:e33887. PONE-D-12-00698 [pii]. 10.1371/journal.pone.0033887 [PubMed: 22470487]

5. Squiban B, Belougne J, Ewbank J, Zugasti O. Quantitative and automated high-throughput genome-wide RNAi screens in *C. elegans*. J Vis Exp. 2012; 60:e3448.10.3791/3448

6. Kamath RS, et al. Systematic functional analysis of the *Caenorhabditis elegans* genome using RNAi. Nature. 2003; 421:231–237. [PubMed: 12529635]

7. Rual JF, et al. Toward improving *Caenorhabditis elegans* phenome mapping with an ORFeome-based RNAi library. Genome Res. 2004; 14:2162–2168. [PubMed: 15489339]

8. Xu S, Chisholm AD. A Galpha(q)-Ca(2+) signaling pathway promotes actin-mediated epidermal wound closure in *C. elegans*. Curr Biol. 2011; 21:1960–1967.10.1016/j.cub.2011.10.050 [PubMed: 22100061]

Author Manuscript Author Manuscript Author Manuscript Author Manuscript

9. Melo JA, Ruvkun G. Inactivation of conserved *C. elegans* genes engages pathogen- and xenobiotic-associated defenses. Cell. 2012; 149:452–466. S0092-8674(12)00346-7 [pii]. 10.1016/j.cell.2012.02.050 [PubMed: 22500807]

10. Hobert O. PCR fusion-based approach to create reporter gene constructs for expression analysis in transgenic *C. elegans*. Biotechniques. 2002; 32:728–730. [PubMed: 11962590]

11. Stringham E, Pujol N, Vandekerckhove J, Bogaert T. *unc-53* controls longitudinal migration in *C. elegans*. Development. 2002; 129:3367–3379. [PubMed: 12091307]

12. Pujol N, et al. A reverse genetic analysis of components of the Toll signalling pathway in *Caenorhabditis elegans*. Curr Biol. 2001; 11:809–821. [PubMed: 11516642]

13. Reddy KC, Andersen EC, Kruglyak L, Kim DH. A polymorphism in *npr-1* is a behavioral determinant of pathogen susceptibility in *C. elegans*. Science. 2009; 323:382–384. [PubMed: 19150845]

14. Jansson HB. Attraction of nematodes to endo-parasitic nematophagous fungi. Trans Brit Mycol Soc. 1982; 79:25–29.

15. Pulak R. Techniques for analysis, sorting, and dispensing of *C. elegans* on the COPAS flow-sorting system. Methods Mol Biol. 2006; 351:275–286. 1-59745-151-7:275 [pii]. 10.1385/1-59745-151-7:275 [PubMed: 16988441]

16. von Reuss SH, et al. Comparative metabolomics reveals biogenesis of ascarosides, a modular library of small-molecule signals in *C. elegans*. J Am Chem Soc. 2012; 134:1817–1824.10.1021/ja210202y [PubMed: 22239548]

17. Pujol N, et al. Anti-fungal innate immunity in *C. elegans* is enhanced by evolutionary diversification of antimicrobial peptides. PLoS Pathog. 2008; 4:e1000105.10.1371/journal.ppat.1000105 [PubMed: 18636113]

Author Manuscript Author Manuscript Author Manuscript Author Manuscript

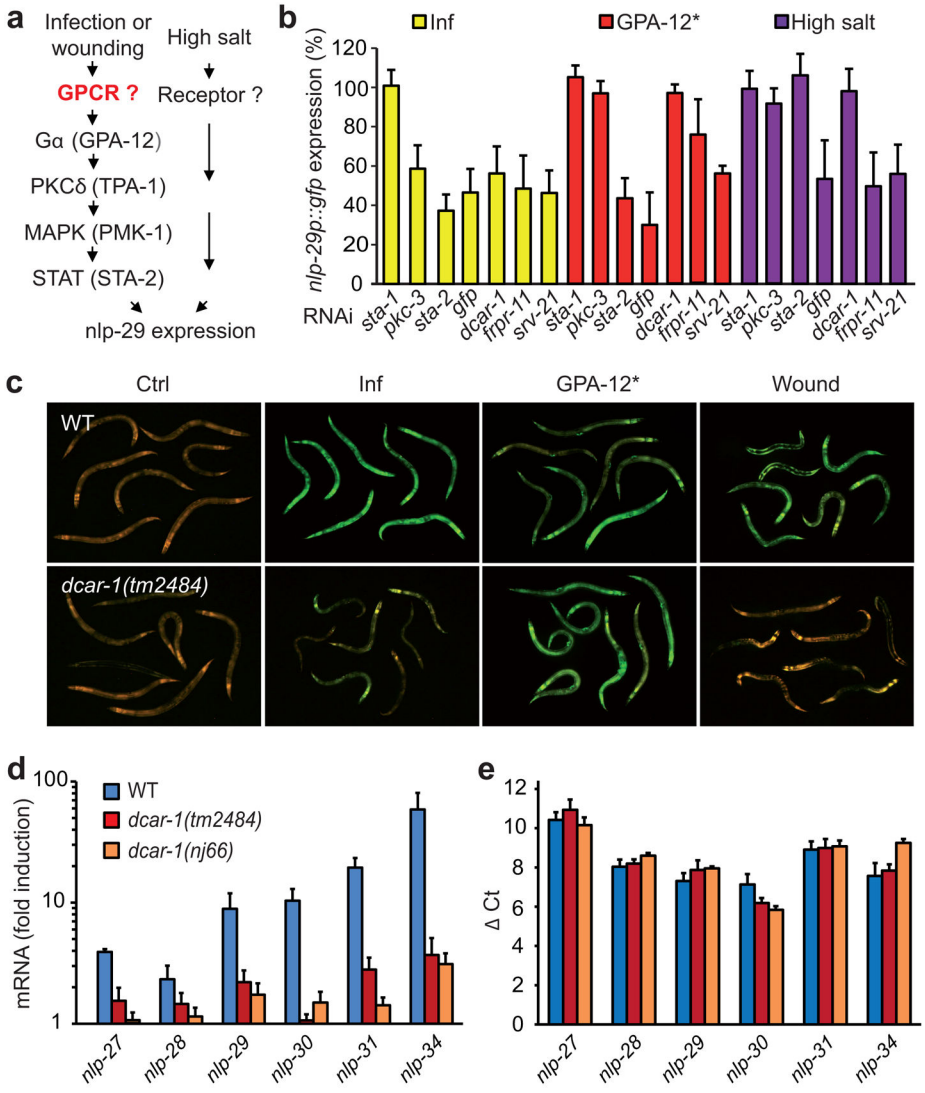


**Figure 1. The GPCR DCAR-1 controls AMP gene expression**

**a,** Simplified scheme of the pathways leading to expression of *nlp-29*. **b**, Relative *nlp-29p::gfp* transgene expression of worms carrying the integrated array *frIs7* treated with RNAi against control or candidate genes and infected by *D. coniospora*, in worms expressing a constitutively active form of GPA-12 (GPA-12*) in the epidermis, or exposed to a high salt medium. The negative control *sta-1*(*RNAi*) does not affect *gfp* expression. Data represent the mean and SD of the normalized GFP fluorescence from a minimum of six biological replicates, with a minimum of 50 worms for each condition. For this and subsequent figures, see online Methods for details of data processing. **c**, Fluorescent images of wild type and *dcar-1(tm2484)* worms carrying *frIs7* after infection by *D. coniospora*, expressing GPA-12* in the epidermis or after wounding. *frIs7* also includes a *col-12p::dsRed* reporter gene; its constitutive expression in the epidermis was unaffected by the different treatments[20]. **d**, Quantitative RT-PCR analysis of the expression of genes in the *nlp-29* cluster in wild-type, *dcar-1(tm2484)* and *dcar-1(nj66)* worms after infection by *D. coniospora*. **e**, Relative abundance of mRNA ($\delta Ct = Ct_{nlp} - Ct_{act-1}$) of genes from the *nlp-29*

cluster in wild-type, *dcar-1(tm2484)* and *dcar-1(nj66)* strains. In **d** and **e**, data are from three independent experiments (average and SD).

Author Manuscript Author Manuscript Author Manuscript Author Manuscript

Author Manuscript Author Manuscript Author Manuscript Author Manuscript

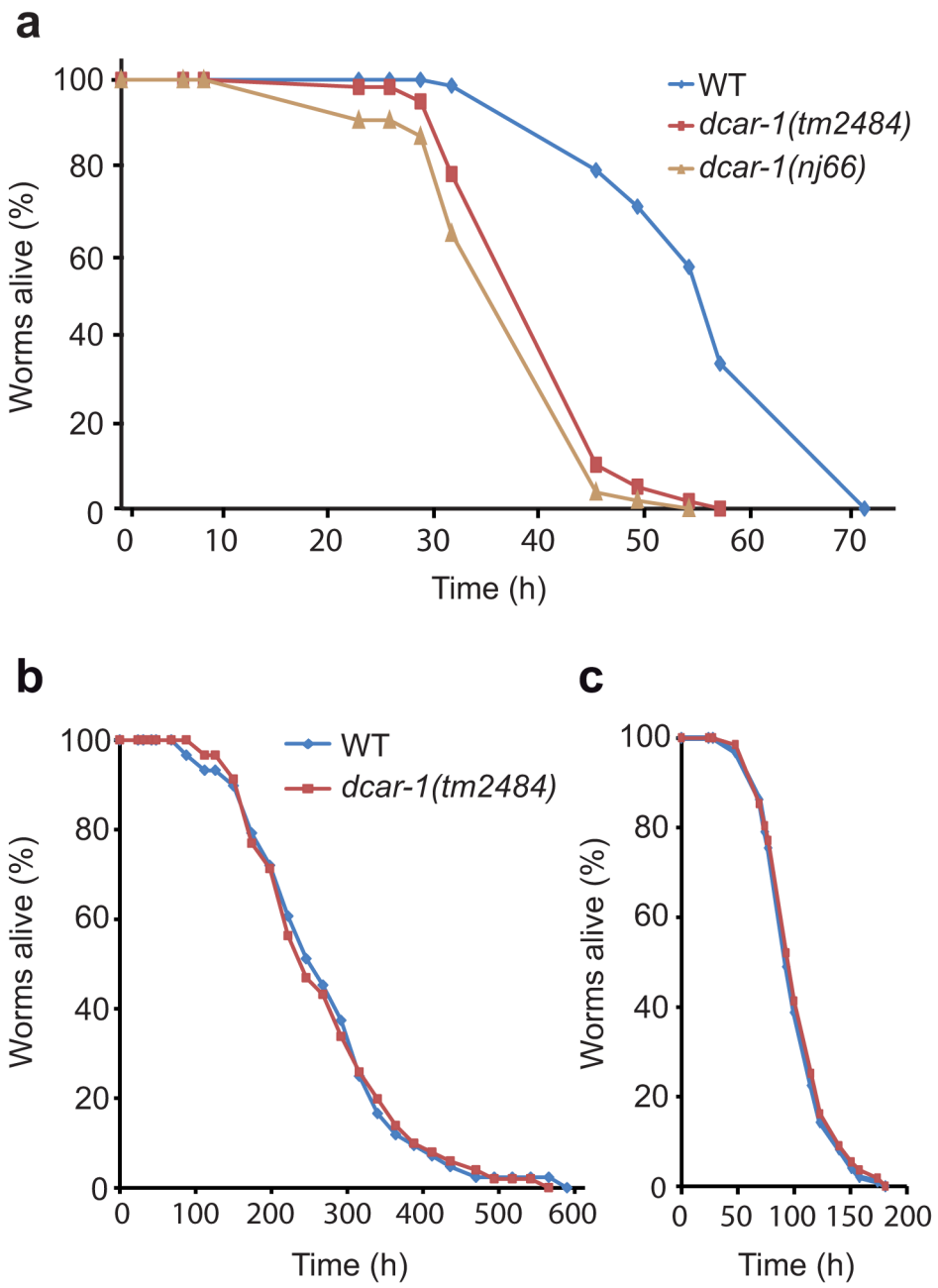


**Figure 2. *dcar-1* specifically controls resistance to fungal infection**

**a**, Survival of wild type (WT), *dcar-1(tm2484)* and *dcar-1(nj66)* worms after infection with *D. coniospora*. (n=72, 60 and 54 respectively) (**a**). The difference between the wild-type and *dcar-1* mutant strains is highly significant ($p<0.0001$; one-sided log rank test). Survival of wild type and *dcar-1(tm2484)* worms on the non-pathogenic *E. coli* strain OP50 (n= 65 for both strains) (**b**) and after infection with *Pseudomonas aeruginosa* PA14 (n= 65 for both strains) (**c**). There is no significant difference between the strains in either assay ($p>0.6$; one-sided log rank test). In all cases, data are representative of three independent experiments.

Author Manuscript Author Manuscript Author Manuscript Author Manuscript

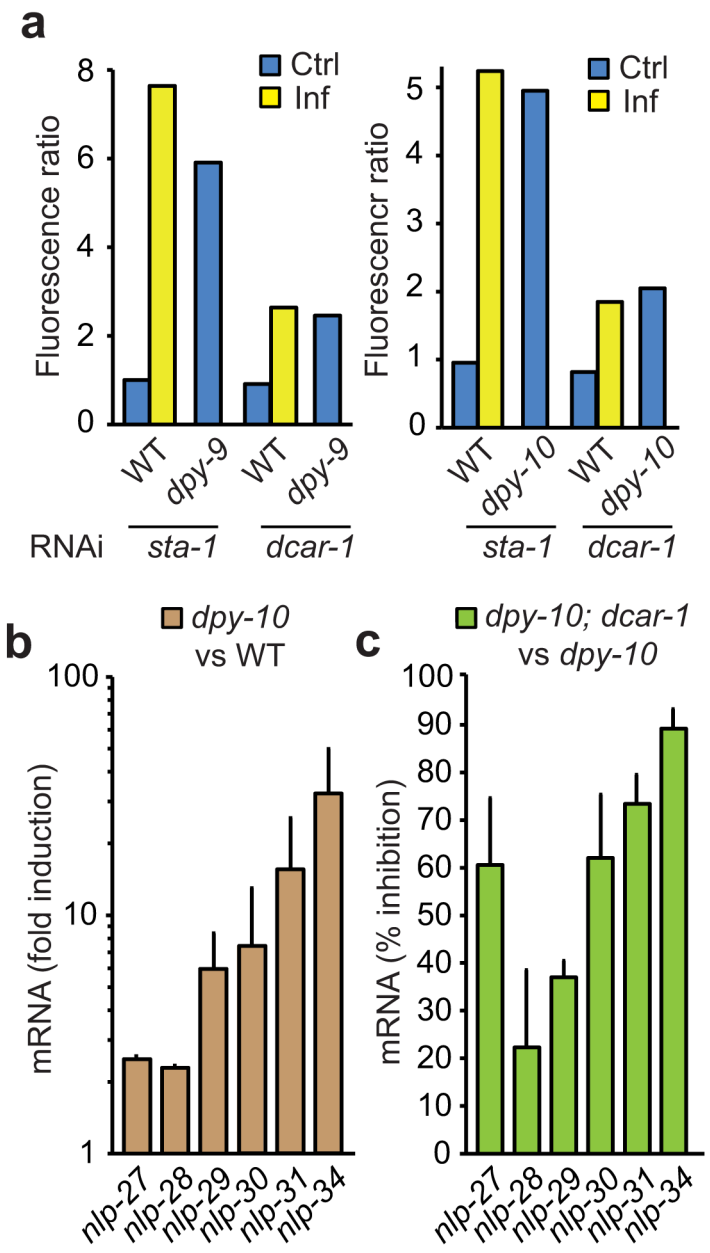


**Figure 3. Elevated AMP gene expression in *dpy-9* and *dpy-10* mutants depends on *dcar-1***

**a**, Normalized fluorescence ratio of wild type, *dpy-9* and *dpy-10* worms carrying *frIs7* treated with RNAi against control *(sta-1)* or *dcar-1*, and infected or not with *D. coniospora*. In this and subsequent figures, for reasons given elsewhere[20], error bars for normalized fluorescence ratios are not shown, but in all cases, the results are representative of at least three biological replicates with a minimum of 50 worms for each condition. **b**,**c**, Relative contributions of *dpy-10* and *dcar-1* to the expression of genes in the *nlp-29* cluster evaluated by quantitative RT-PCR analysis, represented as fold-induction (*dpy-10* vs wild type, (**b**), and % inhibition upon loss of *dcar-1* function (100*(1-($2^{dd}/2^{d}$) (**c**), where *dd* and *d* are the relative abundances (δCt) of each of the 6 *nlp* mRNAs in *dpy-10;dcar-1* and *dpy-10* worms,

respectively. Data are from two technical replicates in two independent experiments (average and SD).

Author Manuscript Author Manuscript Author Manuscript Author Manuscript

Author Manuscript Author Manuscript Author Manuscript Author Manuscript

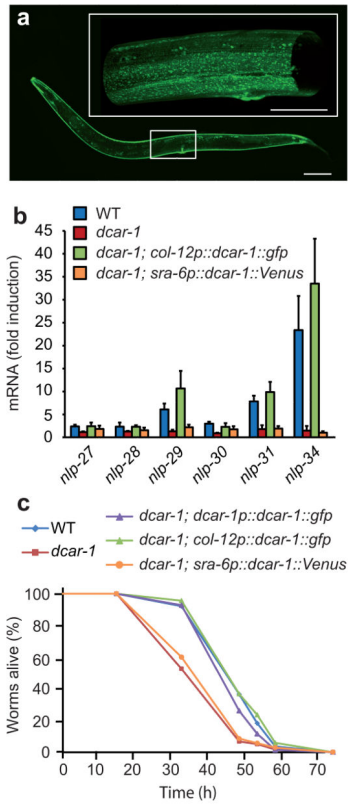


**Figure 4. *dcar-1* acts in the epidermis to regulate *nlp-29* gene expression and resistance to fungal infection**

**a,** Confocal section of a transgenic worm expressing *dcar-1p::dcar-1::gfp* (strain IG1473). A 3D projection reconstructed from 76 optical sections of the boxed region is shown to highlight the expression of *dcar-1p::dcar-1::gfp* on the apical surface in the major epidermal syncytium as reflected by the banded pattern of fluorescence. Scale bar, 50 μm. **b**, Quantitative RT-PCR analysis of the expression of genes in the *nlp-29* cluster in wild-type, *dcar-1(tm2484)*, *dcar-1;col-12p::dcar-1::gfp* and *dcar-1;sra-6p::dcar-1::Venus* mutants worms after infection with *D. coniospora*. Data are from three biological replicates (average and SD). **c,** Survival of wild-type, *dcar-1(tm2484)*, *dcar-1;dcar-1p::dcar-1::gfp*, *dcar-1;col-12p::dcar-1::gfp* and *dcar-1;sra-6p::dcar-1::Venus* mutants worms after infection with *D. coniospora*. For the experiment shown here, n= 65, 67, 68, 71 and 70 respectively). The difference between *dcar-1* and *dcar-1;col-12p::dcar-1::gfp*, and *dcar-1* and *dcar-1p::dcar-1::gfp* are highly significant ($p<0.0001$; one-sided log rank test), while that between *dcar-1* and *dcar-1;sra-6p::dcar-1::Venus* is not ($p=0.44$). The difference in survival between the strains common to the experiments shown in Figs. 2a and 4c is linked to a variation in pathogenicity between different preparations of fungal spores used in experiments performed on different days.

Author Manuscript Author Manuscript Author Manuscript Author Manuscript

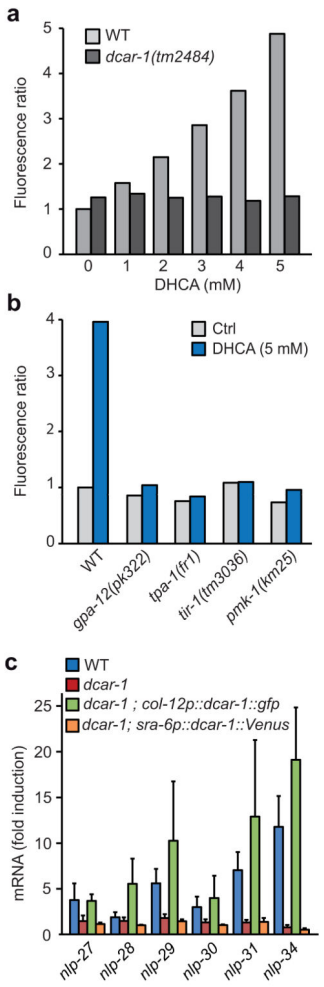


**Figure 5. DHCA mimics the effect of infection on AMP gene expression**

**a–b,** Normalized fluorescence ratio of wild type and mutant worms (a minimum of 50 worms for each condition) carrying *frIs7* treated with increasing concentrations of DHCA (**a**) or a 5 mM solution of DHCA used with wild type and different mutant *C. elegans* strains (**b**). **c** Quantitative RT-PCR analysis of the expression of genes in the *nlp-29* cluster in wild-type, *dcar-1(tm2484)*, *dcar-1;col-12p::dcar-1::gfp* and *dcar-1;sra-6p::dcar-1::Venus* mutant worms following exposure to 5 mM DHCA for 2 hours. Data are from three biological replicates (average and SD).

Author Manuscript Author Manuscript Author Manuscript Author Manuscript

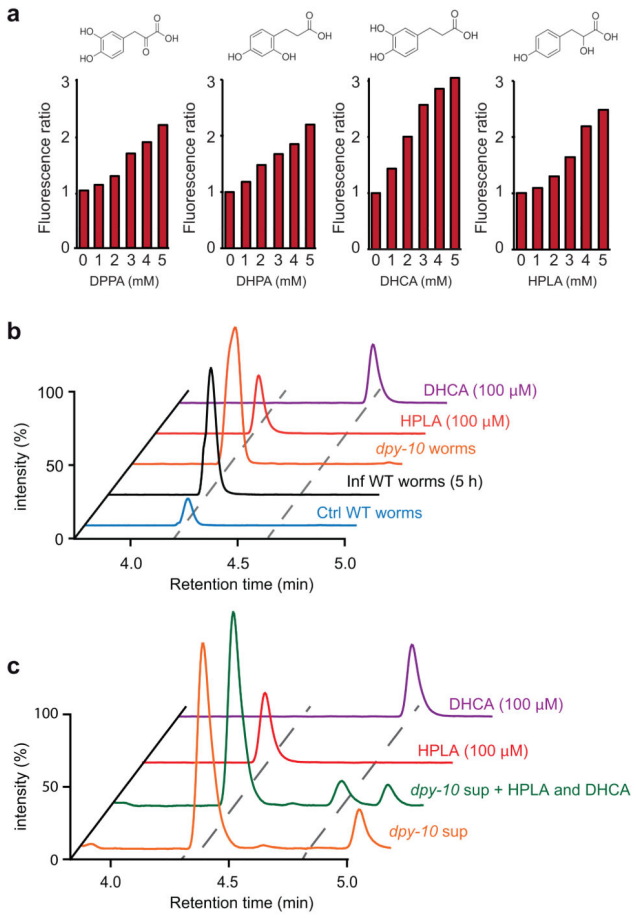


**Figure 6. Identification of HPLA as a potential ligand of DCAR-1**

Chemical structures of 3,4-dihydroxy-phenyl pyruvate (DPPA), 3-(2,4-dihydroxyphenyl) propionic acid (DHPA), dihydrocaffeic acid (DHCA) and 3,4-hydroxyphenyl lactic acid (HPLA), together with normalized fluorescence ratio of young adult wild type worms carrying *frIs7* treated for 2 h at 25°C with increasing concentrations of the indicated chemical. Data are representative of at least three independent experiments with a minimum of 50 worms for each condition. Concentrations of DHCA above 5 mM did not induce a higher level of fluorescence; beyond 80 mM, it was toxic. Concentrations of DPPA, DHPA and HPLA above 5 mM did not induce a higher level of fluorescence; beyond 10 mM, they were toxic. DHCA was previously found to act as a strong DCAR-1 ligand in a *Xenopus* oocyte system. **b**, Comparison of HPLC-MS retention times and relative peak intensities ($ESI^-$, ion chromatogram for *m/z* = 181) of extracts from synchronized young adult *C. elegans* wild-type (WT) worms (blue), 5 h after infection (black), *dpy-10* mutants (orange), synthetic HPLA (red), and synthetic DHCA (magenta). The amount of HPLA increased ~3.5-fold upon infection compared to controls; DHCA was not observed in any sample. **c**, Comparison of retention times (ESI-, ion chromatogram for *m/z* = 181) of natural HPLA in extracts of the supernatant from liquid cultures of *dpy-10* (orange), synthetic HPLA (red), synthetic DHCA (purple), and a mixture of the natural and synthetic samples (green). The

Author Manuscript Author Manuscript Author Manuscript Author Manuscript

HPLC-retention time of synthetic HPLA matches that of natural HPLA, and is distinctly different from the retention time of synthetic DHCA.

Author Manuscript Author Manuscript Author Manuscript Author Manuscript

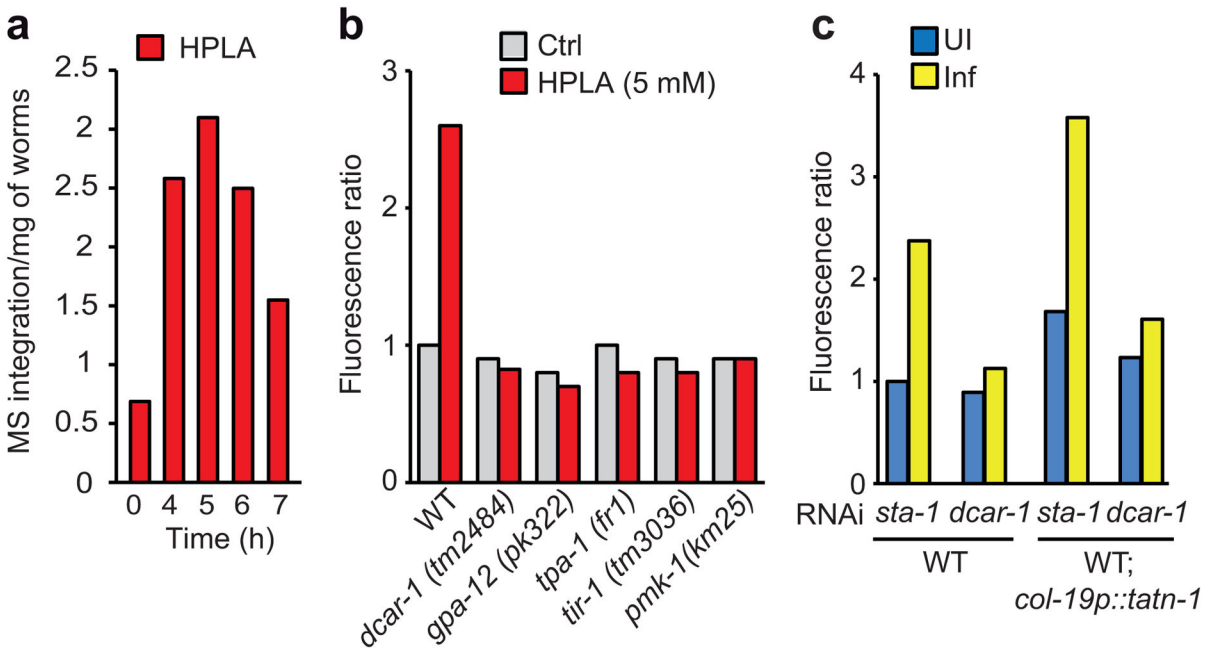


**Figure 7. Endogenous HPLA increases upon infection with *D. coniospora* and trigger *nlp-29* AMP gene expression via a DCAR-1-PMK-1 signalling pathway**

**a**, Abundance of HPLA in control and infected wild-type worms. The abundance of HPLA is represented by HPLC-MS peak integrations (ESI-, ion chromatogram for *m/z* = 181), normalized by the worm pellet dry weight obtained for each condition. **b, c** Normalized fluorescence ratio of wild-type and mutant worms carrying *frIs7* treated with 5 mM of HPLA (**b**) or in wild-type worms that additionally carry an epidermally-expressed construct *col-19p::tatn-1*, infected or not, and subject to RNAi with control or *dcar-1*-targeting clones (**c**). Data are representative of at least 3 (**b**) or 2 (**c**) biological replicates with a minimum of 50 worms for each condition.